THE ARCHIVE OF MECHANICAL ENGINEERING

VOL. LVI 2009 Number 1

DOI: 10.24425/ame.2009.132087

Key words: A-frame, dynamics, modelling, optimisation, stabilization of position

Iwona Adamiec-Wójcik [*], *Paweł Fałat* [**], *Andrzej Maczyński* [***], *Stanisław Wojciech* [****]

LOAD STABILISATION IN AN A-FRAME – A TYPE OF AN OFFSHORE CRANE

The paper presents the dynamic model of an A-frame, which is a kind of an offshore crane with a portal construction. The rigid finite element method (RFEM) has been used in discretization of the flexible substructure. An application of optimisation methods to define the drive function course of the hoisting winch is presented. The goal of the optimisation is to ensure stabilization of the load's position. In order to achieve appropriate numerical effectiveness, the optimisation problem has been solved for a simplified model of an A-frame. Comparison of numerical results obtained for different types of objective functions and types of drive functions is presented in the paper as well.

1. Introduction

Penetration and exploration of the sea floor is one of the modern methods of civilizational expansion. Much of the petroleum and gas consumed by humanity comes from undersea pools. Moreover, many oil and gas pipes, as well as telecommunication cables, are nowadays laid on the sea floor. Therefore, different deep-sea operations requiring sensitive accuracy (e.g. rigging) must be performed more frequently. These operations are often done from ships by using offshore cranes. Because the sea waves cause a motion of the structure of the crane, the stabilisation and positioning of the load is an important task in the design of such cranes. One possible example of this

[*] *University of Bielsko-Biała, Faculty of Management and Computer Science, Willowa 2, 43-309 Bielsko-Biała, Poland; E-mail: i.adamiec@ath.eu*

[**] *University of Bielsko-Biała, Faculty of Management and Computer Science, Willowa 2, 43-309 Bielsko-Biała, Poland; E-mail: falat@ath.eu*

[***] *University of Bielsko-Biała, Faculty of Management and Computer Science, Willowa 2, 43-309 Bielsko-Biała, Poland; E-mail: amaczynski@ath.eu*

[****] *University of Bielsko-Biała, Faculty of Management and Computer Science, Willowa 2, 43-309 Bielsko-Biała, Poland; E-mail: swojciech@ath.eu*

issue is the problem concerned with controlling the position of the cage of a deep-sea remote operating vehicle (ROV) presented by Driscoll et al. [3]. It is important to notice that such vehicles operate at depths up to several thousands meters.

There are many papers where dynamics and control of classical offshore cranes with jib are considered, e. g. Li and Balachandran [12], Ellermann et al. [4], Masoud et. al. [14]. A-frames are hardly ever a topic of scientific papers. A-frames are produced on individual orders, but their significance in trans-shipment, especially deep-sea operations, is undeniable. Dynamics and control of this kind of cranes have been discussed in a doctoral thesis [5].

In the paper, two dynamic models of an A-frame are presented. In the first one, the flexibility of a frame is taken into account, while in the second one this flexibility is omitted. In both cases, the flexibility of rope is considered. The classical rigid finite element method (RFEM) has been used to discretise the frame. The algorithm of optimisation of the drive function for the drum of the hoisting winch is proposed. The goal of the optimisation is to ensure the stabilization of the load's position, i.e. to hold it at the required depth regardless of the ship's motion. In order to achieve appropriate numerical effectiveness, the optimisation problem has been solved using a simplified model of an A-frame.

2. A-frame model

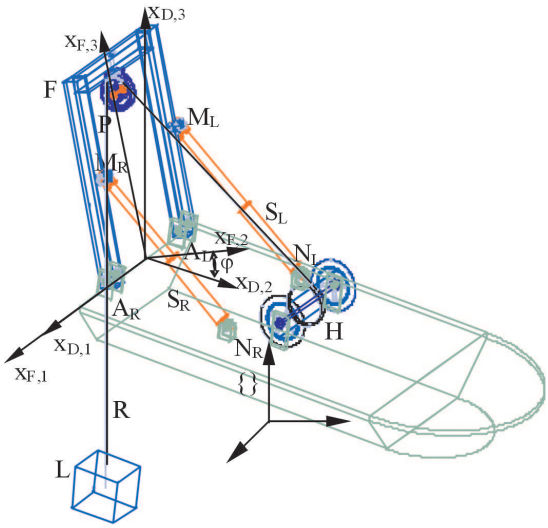

Fig. 1. A-frame scheme

The scheme of an A-frame and the most important points of it are presented in Fig. 1. The following denotations are used: F – supporting structure, P – pulley, R – rope, H – drum of the hoisting winch, L – load, S_R, S_L – right and left servomotor forces, N_R, N_L – connection points of servomotors to the A-frame, A_R, A_L – connection points of the A-frame to the deck, $x_{F,1}$,$x_{F,2}$,$x_{F,3}$ and $x_{D,1}$,$x_{D,2}$,$x_{D,3}$ – coordinate systems assigned to the supporting structure (frame) and to the deck, respectively.

In the formulation of equations of motion of the system (A-frame), homogeneous coordinates and transformations have been used (presented in details in Craig [2]). In this method, coordinates of point P determined in the coordinate system $\{A\}$ can be expressed in coordinate system $\{B\}$ (Fig. 2.) as:

$$\mathbf{r}_B = {}^B_A\mathbf{T}\,\mathbf{r}_A, \tag{1}$$

where $\mathbf{r}_A = \begin{bmatrix} x_{A1} & x_{A2} & x_{A3} & 1 \end{bmatrix}^T$ – vector of coordinates of point P in system $\{A\}$,

$\mathbf{r}_B = \begin{bmatrix} x_{B1} & x_{B2} & x_{B3} & 1 \end{bmatrix}^T$ – vector of coordinates of point P in system $\{B\}$,

${}^B_A\mathbf{T} = \begin{bmatrix} {}^B_A\mathbf{R} & \mathbf{r}_0^{A/B} \\ \mathbf{0} & 1 \end{bmatrix}$ – matrix of transformation,

$\mathbf{r}_0^{A/B} = \begin{bmatrix} x_1^{A/B} & x_2^{A/B} & x_3^{A/B} \end{bmatrix}^T$ – vector describing the position of the origin of coordinate system $\{A\}$ in system $\{B\}$,

${}^B_A\mathbf{R}$ – matrix of rotation.

Euler's angles ZYX have been used to describe the orientation of system $\{A\}$ with respect to $\{B\}$. The choice of angles describing this orientation influences the form of the rotation matrix ${}^B_A\mathbf{R}$.

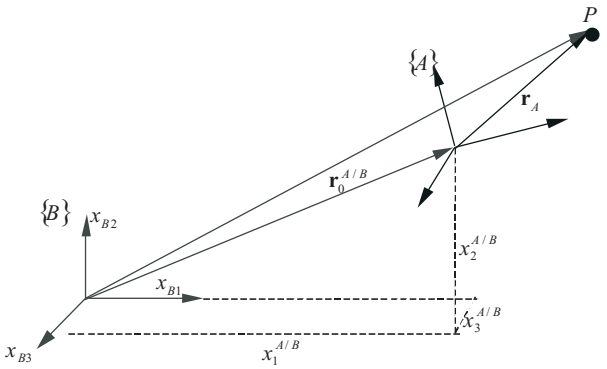

Fig. 2. Coordinate transformation from the system $\{A\}$ to $\{B\}$

Detailed forms of transformation and rotational matrices for the model have been presented in [5].

The frame is the main element of the supporting structure in such cranes. In order to discretise the frame, the rigid finite element method can be applied. The rigid finite element method is presented by Kruszewski et al. [11] and Wittbrodt et al. [15]. Let us consider a prismatic beam. First, the beam of length L is divided into m sections of equal length. Flexible features of the elements are concentrated in spring-damping elements (sdes), which are placed in the middle of the elements of length Δ (Fig. 3a). In the secondary division, the flexible link is replaced by m+1 rigid finite elements (rfes) numbered from 0 to m, and m sdes numbered from 1 to m (Fig. 3b).

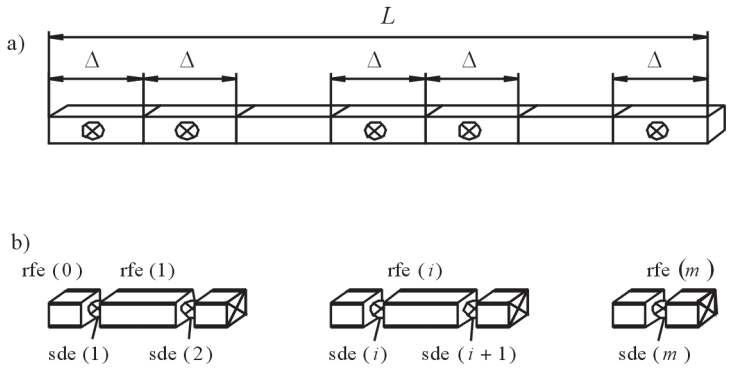

Fig. 3. Discretisation of a beam: a) primary division into elements with finite dimension in order to determine parameters of sdes, b) secondary division

The basic parameters of the sde are values characterising spring and damping features. These are, for spring features of the sde, three coefficients of translational stiffness and three coefficients of rotational stiffness. The damping features of the sde are also defined by three coefficients of translational damping and three coefficients of rotational damping. The stiffness and damping coefficients of the sde, in which all such features of a beam segment with length Δ are concentrated, are determined on the basis of the assumption that a real segment of the beam will deform in the same way and with the same velocities of deformation as the equivalent sde under the same load. The detailed considerations for a prismatic beam are presented in [15]. There the Kelvin-Voigt rheological model is used. For translational and rotational coefficients the following formulae are obtained (Fig. 4):

$$c_{x_1} = \frac{EA}{\Delta}, \quad d_{x_1} = \frac{\eta A}{\Delta}, \tag{2}$$

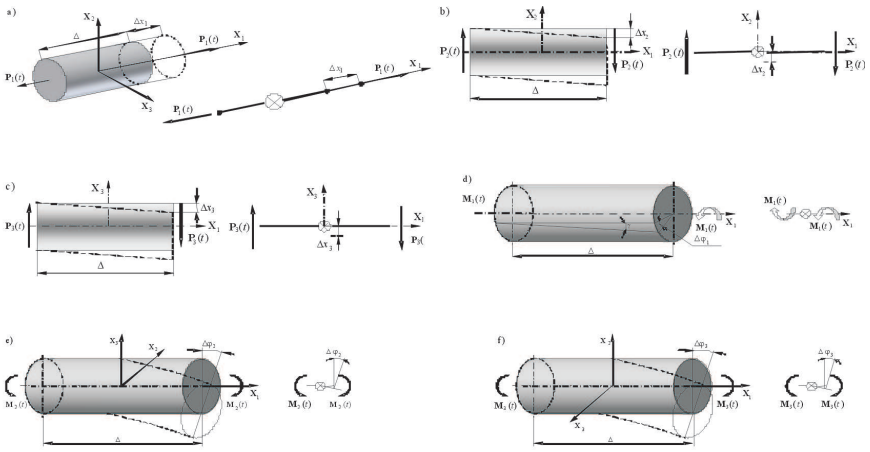

Fig. 4. Sde equivalent to features of one segment from primary division of a beam: a) longitudinal; b, c) shear; d) torsional

$$c_{x_2} = \frac{GA}{\kappa_2 \Delta}, \quad d_{x_2} = \frac{\overline{\eta} A}{\kappa_2 \Delta}, \tag{3}$$

$$c_{x_3} = \frac{GA}{\kappa_3 \Delta}, \quad d_{x_3} = \frac{\overline{\eta} A}{\kappa_3 \Delta}, \tag{4}$$

$$c_{\varphi_1} = \frac{GJ_0}{\Delta}, \quad d_{\varphi_1} = \frac{\overline{\eta} J_0}{\Delta}, \tag{5}$$

$$c_{\varphi_2} = \frac{GJ_2}{\Delta}, \quad d_{\varphi_2} = \frac{\overline{\eta} J_2}{\Delta}, \tag{6}$$

$$c_{\varphi_3} = \frac{GJ_3}{\Delta}, \quad d_{x_3} = \frac{\overline{\eta} J_3}{\Delta}, \tag{7}$$

where E is Young's modulus,

A is cross-section,

η is normal damping material constant,

G is shear modulus (Kirchhoff's modulus),

$\overline{\eta}$ is a material constant of tangential damping,

κ_2, κ_3 are coefficients of cross-section shape, e.g. for a rectangular cross-section this coefficient is equal 1.2,

J_0 is polar moment of inertia of a cross section,

J_2, J_3 are second area moments of inertia of a cross-section with respect to axis x_2 and x_3.

More information, also for other shapes of cross-section e. g. open profiles, can be found in [15] and [11].

In our previous works [5] and [8], at first three beams were distinguished (right-1, top-2, left-3) in the frame. Thus, the subsystems modelled have been treated as rectilinear beams with constant or variable cross section. Then, each beam was divided into rigid finite elements and spring-damping elements, Fig. 5. This necessitates taking into account the reaction forces and moments at points B_L and B_R, and increases the number of constraint equations. This approach is described in [5].

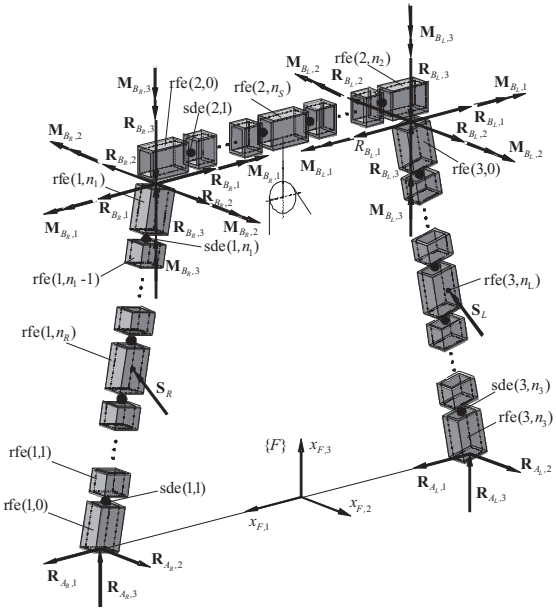

Fig. 5. A-frame divided into three beams which were divided into rfes and sdes

In this paper, we present a different approach. The frame is treated as one beam, which is divided into rfes and sdes. The obtained chain of rfes and sdes is presented in Fig. 6.

The position of each rfe of the undeformed beam is defined by the coordinate system ${}^{E}\{i\}$ with respect to the coordinate system $\{0\}$ of rfe 0, by a transformation matrix with constant components:

$$ {}^{0}_{E}\mathbf{T}_i = \begin{bmatrix} {}^{0}_{E}\mathbf{\Theta}_i & {}^{0}_{E}\mathbf{s}_i \\ \mathbf{0} & 1 \end{bmatrix}, \tag{8} $$

where ${}^{0}_{E}\mathbf{\Theta}_i$ is the matrix of cosines of the system ${}^{E}\{i\}$ with respect to $\{0\}$, and ${}^{0}_{E}\mathbf{s}_i$ is the vector of coordinates of the origin of the system ${}^{E}\{i\}$ in $\{0\}$ (Fig. 7). The coordinate system $\{i\}$ rigidly attached to the i^{th} rfe moves together with rfe i when the beam is deformed. Its position in the coordinate

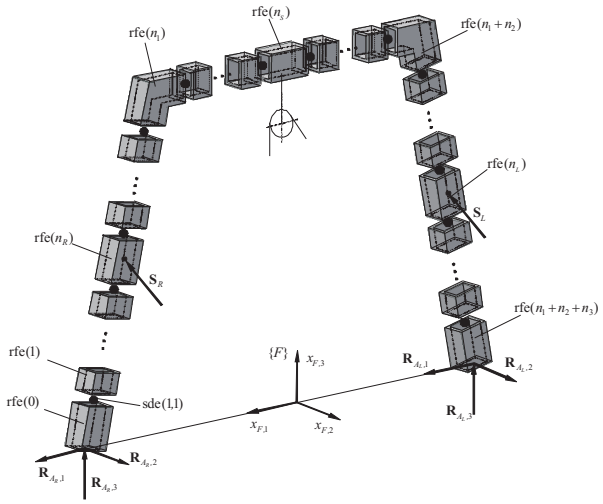

Fig. 6. A-frame as one beam, and its division into rfes and sdes

system ${}^{E}\{i\}$ is defined by generalized coordinates of the i^{th} element, which are the components of the vector:

$$\mathbf{q}_i = \begin{bmatrix} \mathbf{x}_i \\ \boldsymbol{\phi}_i \end{bmatrix}, \tag{9}$$

where $\mathbf{x}_{i,j} = \begin{bmatrix} x_{i,1} & x_{i,2} & x_{i,3} \end{bmatrix}^T$ and $\boldsymbol{\phi}_i = \begin{bmatrix} \varphi_{i,1} & \varphi_{i,2} & \varphi_{i,3} \end{bmatrix}^T$ are vectors of displacements and rotation angles presented in Fig. 7.

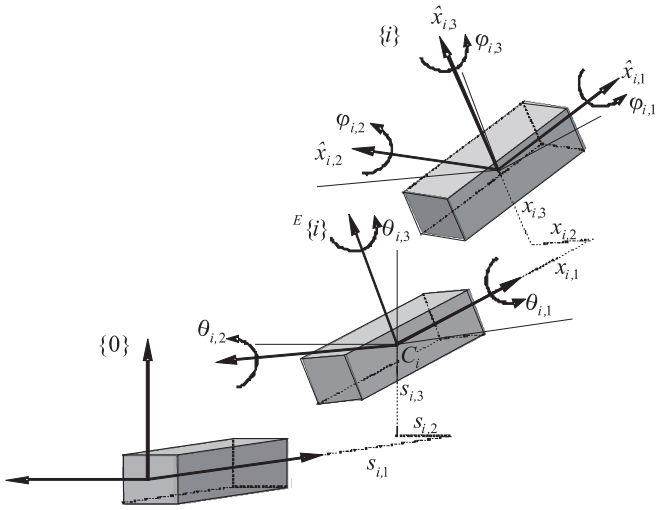

Fig. 7. The systems of i^{th} rfe and generalized coordinates

If we assume that angles $\varphi_{i,j}$ are small, then the transformation matrix from local coordinate system $\{i\}$ to the system ${}^{E}\{i\}$ takes the following form [15]:

$$\mathbf{T}_i = \begin{bmatrix} 1 & -\varphi_{i,3} & \varphi_{i,2} & x_{i,1} \\ \varphi_{i,3} & 1 & -\varphi_{i,1} & x_{i,2} \\ -\varphi_{i,2} & \varphi_{i,1} & 1 & x_{i,3} \\ 0 & 0 & 0 & 1 \end{bmatrix} = \mathbf{I} + \sum \mathbf{D}_j q_{i,j}, \tag{10}$$

where $\left.\begin{matrix} q_{i,j} = x_{i,j} \\ q_{i,j+3} = \varphi_{i,j} \end{matrix}\right\}$ for $j = 1, 2, 3,$

$$\mathbf{D}_1 = \begin{bmatrix} 0 & 0 & 0 & 1 \\ 0 & 0 & 0 & 0 \\ 0 & 0 & 0 & 0 \\ 0 & 0 & 0 & 0 \end{bmatrix}, \quad \mathbf{D}_2 = \begin{bmatrix} 0 & 0 & 0 & 0 \\ 0 & 0 & 0 & 1 \\ 0 & 0 & 0 & 0 \\ 0 & 0 & 0 & 0 \end{bmatrix}, \quad \mathbf{D}_3 = \begin{bmatrix} 0 & 0 & 0 & 0 \\ 0 & 0 & 0 & 0 \\ 0 & 0 & 0 & 1 \\ 0 & 0 & 0 & 0 \end{bmatrix},$$

$$\mathbf{D}_4 = \begin{bmatrix} 0 & 0 & 0 & 0 \\ 0 & 0 & -1 & 0 \\ 0 & 1 & 0 & 0 \\ 0 & 0 & 0 & 0 \end{bmatrix}, \quad \mathbf{D}_5 = \begin{bmatrix} 0 & 0 & 1 & 0 \\ 0 & 0 & 0 & 0 \\ -1 & 0 & 0 & 0 \\ 0 & 0 & 0 & 0 \end{bmatrix}, \quad \mathbf{D}_6 = \begin{bmatrix} 0 & -1 & 0 & 0 \\ 1 & 0 & 0 & 0 \\ 0 & 0 & 0 & 0 \\ 0 & 0 & 0 & 0 \end{bmatrix}.$$

The transformation matrix $\mathbf{B}_i$ that allows us to transform coordinates from the local coordinate system $\{i\}$ to the inertial coordinate system $\{\}$ according to the relation:

$$\mathbf{r} = \mathbf{B}_i \, \mathbf{r}_i, \tag{11}$$

where $\mathbf{r}_i$ is a vector of coordinates in local system $\{i\}$,
$\mathbf{r}$ is a vector of coordinates in base system $\{\}$,
has the form:

$$\mathbf{B}_i = \mathbf{B}_i(t, \mathbf{q}_i) = \mathbf{T}_D \, \mathbf{T}_F \, {}^{0}_{E}\mathbf{T}_i \, \mathbf{T}_i = \mathbf{A}(t) \, \mathbf{P}_i(\mathbf{q}_i), \tag{12}$$

where $\mathbf{T}_D = \mathbf{T}_D(t)$ defines the motion of the ship deck with respect to base system $\{\}$,
$\mathbf{T}_F = \mathbf{T}_F(\varphi(t))$ describes the rotation of the frame in the coordinate system of the deck $\{D\}$,
${}^{0}_{E}\mathbf{T}_i = \text{const}$ is defined in (8),
$\mathbf{T}_i = \mathbf{T}_i(\mathbf{q}_i)$ has the form presented in (10),

$\mathbf{A}(t) = \mathbf{T}_D\,\mathbf{T}_F$,
$\mathbf{P}_i = {}^{0}_{E}\mathbf{T}_i\,\mathbf{T}_i$.

In the case when the axes of local coordinate system $\{i\}$ are chosen as principal central axes of the rfe, the mass and inertial features of the i^{th} rfe are defined by: m_i its mass, and $J_{i,j}\,(j = 1,\ 2,\ 3)$ which are mass moments of inertia with respect to axis $\mathbf{X}_{i,j}$.

The equations of motion of the system considered can be obtained from Lagrange equations. This approach requires the kinetic and potential energy of the system to be defined. The kinetic energy of the i^{th} rfe can be calculated as:

$$E_i = \frac{1}{2}\mathrm{tr}\{\dot{\mathbf{B}}_i\,\mathbf{H}_i\,\dot{\mathbf{B}}_i^T\}, \tag{13}$$

where $tr\{\}$ denotes the trace of matrix $\{\}$,

$\mathbf{H}_i$ is the pseudo-inertia matrix defined in [15].

Following the considerations presented in [15], one can obtain:

$$\frac{d}{dt}\frac{\partial E_i}{\partial \dot{\mathbf{q}}_i} - \frac{\partial E_i}{\partial \mathbf{q}_i} = \mathbf{M}_i\ddot{\mathbf{q}}_i + \mathbf{e}_i, \tag{14}$$

where $\mathbf{M}_i = \mathrm{diag}\{m_i,\ m_i,\ m_i, J_{i,1},\ J_{i,2},\ J_{i,3}\}$,

$$e_{i,j} = e_{i,j}(t,\ \mathbf{q}_i,\ \dot{\mathbf{q}}_i) = \mathrm{tr}\left\{\mathbf{B}_{i,j}\mathbf{H}_i\left[\ddot{\mathbf{A}}\mathbf{P}_i + 2\dot{\mathbf{A}}\dot{\mathbf{P}}_i\right]^T\right\},$$

$$\mathbf{B}_{i,j} = \mathbf{A}\,\frac{\partial \mathbf{P}_i}{\partial q_{i,j}}, \qquad \frac{\partial \mathbf{P}_i}{\partial q_{i,j}} = {}^{0}_{E}\mathbf{T}_i\mathbf{D}_j = \mathrm{const.}$$

The kinetic energy of the frame is:

$$E = \sum_{i=0}^{n} E_i, \tag{15}$$

where $n = n_1 + n_2 + n_3 + 1$, and it is possible to calculate:

$$\frac{d}{dt}\frac{\partial E}{\partial \dot{\mathbf{q}}_F} - \frac{\partial E}{\partial \mathbf{q}_F} = \mathbf{M}_F\ddot{\mathbf{q}}_F + \mathbf{e}_F, \tag{16}$$

where $\mathbf{M}_F = \mathrm{diag}\{\mathbf{M}_0,\ \ldots,\ \mathbf{M}_n\}$,

$$\mathbf{e}_F = \left[\mathbf{e}_0^T\ \ldots\ \mathbf{e}_n^T\right]^T, \quad \mathbf{q}_F = \left[\mathbf{q}_0^T\ \ldots\ \mathbf{q}_n^T\right]^T.$$

The potential energy of deformation of sdes can be expressed as follows [11]:

$$V_F = \frac{1}{2}\mathbf{q}_F^T \mathbf{K}_F \mathbf{q}_F, \tag{17}$$

where $\mathbf{K}_F$ is the stiffness matrix with constant coefficients. Similarly, one can calculate the dissipation of energy as:

$$D_F = \frac{1}{2}\dot{\mathbf{q}}_F^T \mathbf{L}_F \dot{\mathbf{q}}_F, \tag{18}$$

where $\mathbf{L}_F$ is the damping matrix with constant elements. From what has been written above, one can calculate:

$$\frac{\partial V_F}{\partial \mathbf{q}_F} = \mathbf{K}_F \mathbf{q}_F, \tag{19}$$

$$\frac{\partial D_F}{\partial \dot{\mathbf{q}}_F} = \mathbf{L}_F \dot{\mathbf{q}}_F. \tag{20}$$

The potential energy of gravity forces of the frame can be calculated as:

$$V_g^F = \sum_{i=0}^{n} m_i g\, \boldsymbol{\theta}_3\, \mathbf{B}_i\, \mathbf{r}_{C,i}, \tag{21}$$

where g is acceleration of gravity,

$$\boldsymbol{\theta}_3 = [\ 0 \quad 0 \quad 1 \quad 0\ ],$$

$$\mathbf{r}_{C,i} = [\ 0 \quad 0 \quad 0 \quad 1\ ].$$

So:

$$\frac{\partial V_g^F}{\partial \mathbf{q}_F} = \mathbf{G}_F, \tag{22}$$

where $\mathbf{G}_F = [\mathbf{G}_0^T \ \ldots \ \mathbf{G}_n^T]$,

$$\mathbf{G}_i = [G_{i,1} \ \ldots \ G_{i,6}],$$

$$\mathrm{G}_{i,j} = m_i\, g\, \boldsymbol{\theta}_3\, \mathbf{D}_j\, \mathbf{r}_{C,i},$$

$\mathbf{D}_j$ is defined in (10).

ENERGY OF LOAD AND DRUM OF THE HOISTING WINCH

The load is modelled as a particle. The vector of its generalized coordinates is expressed in the following form $\mathbf{q}_L = \left[\ x_{L,1} \quad x_{L,2} \quad x_{L,3}\ \right]^T$. The

angle of rotation of the drum of the hoisting winch is denoted as φ_H. Kinetic energy of the load and the drum can then be calculated as:

$$T_R = \frac{1}{2} m_L \dot{r}_L^2 + \frac{1}{2} I_H \dot{\varphi}_H^2, \tag{23}$$

where I_H is the moment of inertia mass of the drum,

$$\dot{r}_L^2 = \dot{x}_{L,1}^2 + \dot{x}_{L,2}^2 + \dot{x}_{L,3}^2.$$

Potential energy of the load is determined as:

$$V_g^L = m_L \, g \, x_{L,3}. \tag{24}$$

ELASTIC DEFORMATION OF THE ROPE

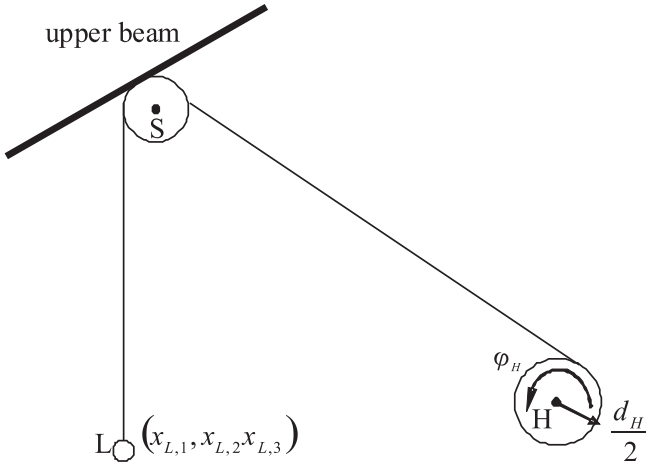

Fig. 8. Rope system

The rope system of the A-frame is presented in Fig. 8. It is assumed that radii of pulleys are small compared to the dimensions of the whole mechanism, and also that the rope passes through points S and H – centres of the pulley and the drum, respectively. Because the radii of pulleys are small and the length of the rope may be hundreds of meters, this simplification can be seen as admissible. Potential energy of elastic deformation of the rope and its dissipation can be expressed in the following forms:

$$V_R = \frac{1}{2} c_R \delta_R \Delta_R^2, \tag{25}$$

$$D_R = \frac{1}{2} d_R \delta_R \dot{\Delta}_R^2, \tag{26}$$

where $\delta_R = \begin{cases} 0 \text{ if } \Delta_R \leq 0 \\ 1 \text{ if } \Delta_R > 0 \end{cases}$,

$$\Delta_R = |LS| + |SH| - l_0 - \varphi_H \frac{d_H}{2},$$

$$|LS| = |\mathbf{r}_L - \mathbf{r}_S|,$$

$$|SH| = |\mathbf{r}_S - \mathbf{r}_H|,$$

$c_R = \dfrac{E_R F_R}{l}$ – stiffness coefficient of the rope,
d_R – damping coefficient of the rope,
l_0, l – initial and current length of the rope, respectively,
E_R – Young's modulus of the rope material,
F_R – cross-section of the rope,
d_H – diameter of the drum.

MOTION EQUATIONS

The vector of A-frame generalised coordinates can be presented in the form:

$$\mathbf{q} = \begin{bmatrix} \mathbf{q}_F \\ \mathbf{q}_R \end{bmatrix}, \tag{27}$$

where $\mathbf{q}_F$ is the vector of generalised coordinates of the discretised frame defined in (16) and vector $\mathbf{q}_R = \begin{bmatrix} x_{L,1} & x_{L,2} & x_{L,3} & \varphi_H \end{bmatrix}^T$ contains generalised coordinates of the load and the angle of rotation of the drum.

Then the equations of motion of the system can be written as:

$$\mathbf{M}\ddot{\mathbf{q}} + \mathbf{L}\dot{\mathbf{q}} + \mathbf{K}\mathbf{q} = \mathbf{Q} + \mathbf{D}\mathbf{R} \tag{28}$$

where $\mathbf{M} = \begin{bmatrix} \mathbf{M}_F & 0 \\ 0 & \mathbf{M}_L \end{bmatrix}$,

$$\mathbf{M}_L = diag\{m_L, m_L, m_L, I_H\},$$

$$\mathbf{L} = \begin{bmatrix} \mathbf{L}_F & 0 \\ 0 & 0 \end{bmatrix}, \quad \mathbf{K} = \begin{bmatrix} \mathbf{K}_F & 0 \\ 0 & 0 \end{bmatrix},$$

$$\mathbf{Q} = \begin{bmatrix} -\dfrac{\partial V_g^F}{\partial \mathbf{q}_F} - \dfrac{\partial V_R}{\partial \mathbf{q}_F} - \dfrac{\partial D_R}{\partial \dot{\mathbf{q}}_F} - \mathbf{e}_F \\ -\dfrac{\partial V_g^L}{\partial \mathbf{q}_R} - \dfrac{\partial V_R}{\partial \mathbf{q}_R} - \dfrac{\partial D_R}{\partial \dot{\mathbf{q}}_R} - \mathbf{e}_L \end{bmatrix},$$

D, **R** are matrix and vector of reaction forces,

$\dfrac{\partial V_R}{\partial \mathbf{q}_F}$, $\dfrac{\partial V_R}{\partial \mathbf{q}_R}$, $\dfrac{\partial D_R}{\partial \dot{\mathbf{q}}_F}$, $\dfrac{\partial D_R}{\partial \dot{\mathbf{q}}_R}$ can be calculated as in [5] and involve non-linear terms.

Forces of reactions on the frame are presented in Fig. 6. Vector **R** of generalised forces then specifically includes:

reaction $\mathbf{R}_{AL} = \begin{bmatrix} R_{AL,1} & R_{AL,2} & R_{AL,3} \end{bmatrix}^T$,

reaction $\mathbf{R}_{AR} = \begin{bmatrix} R_{AR,1} & R_{AR,2} & R_{AR,3} \end{bmatrix}^T$

and forces in servomotors S_L and S_R.

These forces can be written in the vector form:

$$\mathbf{R} = \begin{bmatrix} S_R & S_L & \mathbf{R}_{AR}^T & \mathbf{R}_{AL}^T \end{bmatrix}^T. \tag{29}$$

Finally, the mathematical model of an A-frame has been written in the form of a system of differential equations of the second order (28) and constraint equations in acceleration form:

$$\mathbf{D}^T \ddot{\mathbf{q}} = \mathbf{W}, \tag{30}$$

where $\mathbf{W} = \mathbf{W}(\mathbf{q}, \dot{\mathbf{q}})$.

In these equations, there are: $n_q = \sum_{k=1}^{3} 6(1+n) + 4$ (components of vector **q**) plus $n_R = 2+2\cdot 3 = 8$ (components of vector **R**) unknowns. So, the number of unknowns is equal to the sum of number of equations (28) and (30).

In the method presented, the mass matrix **M** is a diagonal matrix with constant elements. This enables us to apply algorithms presented in [15] and reduce the calculation time.

3. Optimisation problem

One of the major problems connected with the design and control of cranes is the choice of the drive functions which ensure proper motion of the system**.** In the A-frame case, a very important problem is the stabilisation of load position, regardless of motion of the ship caused by sea waves. Using the drive of the drum of the hoisting winch, we can try to solve this problem. Time courses of drive functions can be defined in the optimisation process.

In this paper, the objective function is assumed to be in one of following forms:

$$\Omega_1 = \int_0^{t_k} [x_{L,3} - h]^2 \to \min, \tag{31}$$

$$\Omega_2 = \max_{0 \le t \le t_k} \left| x_{L,3} - h \right| \to \min \tag{32}$$

,

where $x_{L,3}$ is load coordinate,

h is required depth.

This means that one expects that as the result of optimisation the course of function $\varphi_H(t)$ will be obtained which minimises the average or maximal value of deviation of load position from the required amount. During the optimisation process, the parameters of ship hull movement and coordinates of the winch position have been assumed to be known.

In the paper, we assume that function φ_H describes the rotation angle of the winch drum has either the form presented in [5]:

$$\varphi_H(t) = a_i t^3 + b_i t^2 + c_i t + d_i, \quad \text{for } t \in < t_{i-1}, t_i >, \tag{33}$$

where $i = 1, \ldots, m$,

a_i, b_i, c_i, d_i are coefficients taken as shown in [1] for spline functions of the third order,

t_i is point in interval $< 0, t_k >$ (Fig. 9),

or in [13]:

$$\varphi_H(t) = A_0 + \sum_{i=1}^{n} A_i \sin(\omega_i t + \alpha_{i,0}), \quad \text{for } t \in < 0, t_k >, \tag{34}$$

where

A_i – amplitudes,

ω_i – frequencies,

$\alpha_{i,0}$ – phase angles.

As the decisive variables in the optimisation task we can choose:

$$\mathbf{X} = \left[\varphi_H^0, \varphi_H^1, \ldots, \varphi_H^m\right]^T \text{ (see Fig.9)} \tag{35}$$

in case (31), i.e. when spline functions are applied, or:

$$\mathbf{X} = [A_0, A_1, \omega_1, \alpha_{1,0}, \ldots, A_n, \omega_n, \alpha_{n,0}]^T \tag{36}$$

in the case when a pseudo-harmonic response is assumed.

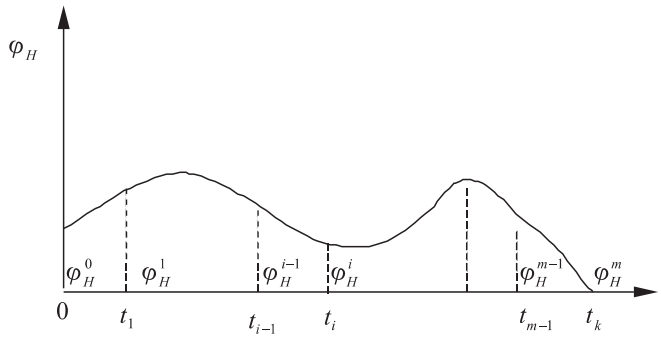

Fig. 9. The decisive variables

In either case, at every step of the optimisation, the equations of motion of the system have to be integrated for $t \in \langle 0, t_k \rangle$ in order to calculate the value of the functional $\Omega_{1,2}$ from (24). Such an approach requires high numerical efficiency in solving A-frame equations of motion. For that reason the optimisation problem has been solved for the simplified model of an A-frame.

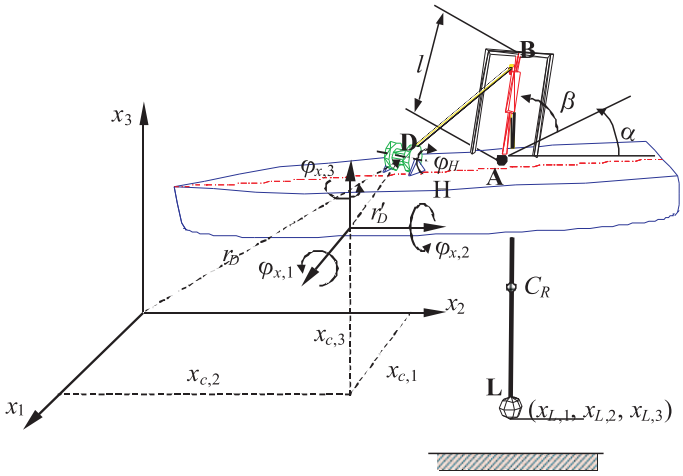

Fig. 10. Scheme of the simplified model

In the simplified model of an A-frame, ideal stiffness of the frame has been assumed. The rope as the most flexible part of the system essentially influences dynamics of the load. Thus, the flexibility of the rope has been taken into consideration. However, it should be underlined that flexibility of the frame and servo-motors can be significant. Doctoral thesis [5] presents problems of stabilization of the load at the given depth where this flexibility is important. However, in some problems, the flexibility of the frame can be neglected, which is the case for the model presented in Fig. 10. The

water damping ratio has not been taken into account. Ship motion has been assumed to be determined, by known functions:

$$\begin{cases} x_{C,1} = x_{C,1}(t) \\ y_{C,2} = y_{C,2}(t) \\ z_{C,3} = z_{C,3}(t) \\ \varphi_{x,1} = \varphi_{x,1}(t) \\ \varphi_{x,2} = \varphi_{x,2}(t) \\ \varphi_{x,3} = \varphi_{x,3}(t) \end{cases}. \tag{37}$$

This means that matrix $\mathbf{T}_D$ from (11) has the form:

$$\mathbf{T}_D = \begin{bmatrix} c\varphi_{x,3}\,c\varphi_{x,2} & c\varphi_{x,3}\,s\varphi_{x,2}\,s\varphi_{x,1} - s\varphi_{x,3}\,c\varphi_{x,1} & c\varphi_{x,3}\,s\varphi_{x,2}\,c\varphi_{x,1} + s\varphi_{x,3}\,s\varphi_{x,1} & x_{C,1} \\ s\varphi_{x,3}\,c\varphi_{x,2} & s\varphi_{x,3}\,s\varphi_{x,2}\,s\varphi_{x,1} + c\varphi_{x,3}\,c\varphi_{x,1} & s\varphi_{x,3}\,s\varphi_{x,2}\,c\varphi_{x,1} - c\varphi_{x,3}\,s\varphi_{x,1} & x_{C,2} \\ -s\varphi_{x,2} & c\varphi_{x,2}\,s\varphi_{x,1} & c\varphi_{x,2}\,c\varphi_{x,1} & x_{C,3} \\ 0 & 0 & 0 & 1 \end{bmatrix}, \tag{38}$$

where $c\varphi$=cosφ and $s\varphi$=sinφ.

The frame angles are assumed to be constant.

Kinetic and potential energies of the system can be expressed in the form:

$$T = \frac{1}{2} m_L \left(\dot{x}_{L,1}^2 + \dot{x}_{L,2}^2 + \dot{x}_{L,3}^2 \right), \tag{39}$$

$$V = \frac{1}{2} \delta_R c_R \Delta_R^2 + m_L g x_{L,3}, \tag{40}$$

$$D = \frac{1}{2} \delta_R d_R \dot{\Delta}_R, \tag{41}$$

where δ_R, c_R, d_R are defined in (26),

$$\Delta_R = |DB| + |BN| - l_0 + \varphi_H r_H.$$

Lagrange's equations of the second order have been used to determine the equations of motion of the system. The details are presented in [6]. These differential equations of the second order have been integrated using the Runge-Kutta method. The Nelder-Meads method has been applied in order to solve the optimisation task.

4. Numerical simulations

It should be mentioned that the numerical model of the A-frame presented in section 2 has been used in the Norwegian company TTS-Aktro from Molde for a fast analysis of forces and stresses at the initial stage of choosing parameters of the system and for cost calculations. In order to verify the model, the results obtained using our program (RFEM) have been compared with those obtained using commercial FEM program (NASTRAN package) [7]. Static analysis has been carried out for a model prepared with a Hyper Mash package using shell elements TRIA3 and QUAD4. Volume elements HEXA8 have been used to model a cylindrical eye of the frame while the connection of the frame with pivoting point has been modelled using CBEAM elements. Calculations carried out using NASTRAN have been much more time consuming in comparison with the authors' programme and it was due to a large number of elements used in discretisation of the frame. There have been compared reactions in joints, stresses and deflections of beams obtained. Some examples are presented in Fig. 11.

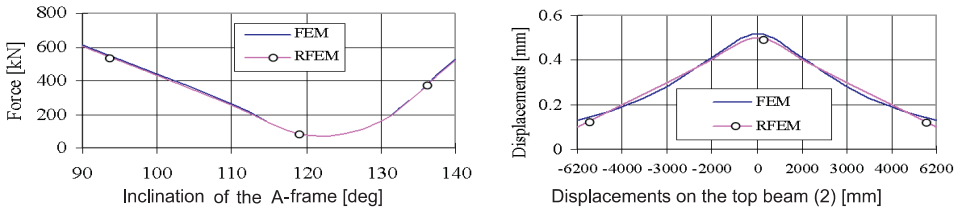

Fig. 11. Comparison of FEM and RFEM models

Dynamic analysis has been carried out by ADAMS-ANSYS package. Primary discretisation of the frame into 1536 SHELL63 elements has been done using ANSYS. Connections of the frame with the deck and servomotors have been modelled using 97 BEAM4 elements. Having performed the modal analysis the model has been transferred to ADAMS. 30 modes have been considered in further calculations. A comparison of the results obtained using RFEM model with those from ADAMS-ANSYS systems in dynamical conditions can be found in [5] and some of them are presented in Fig. 12. Small vibrations seen in the graph are due to the fact that damping has not been taken into account in the numerical model.

Numerical simulations related to the load stabilisation problem have been carried out for the rectangular A-frame with lifting capacity up to 100 Mg. The main geometrical parameters of the crane are presented in Fig. 13.

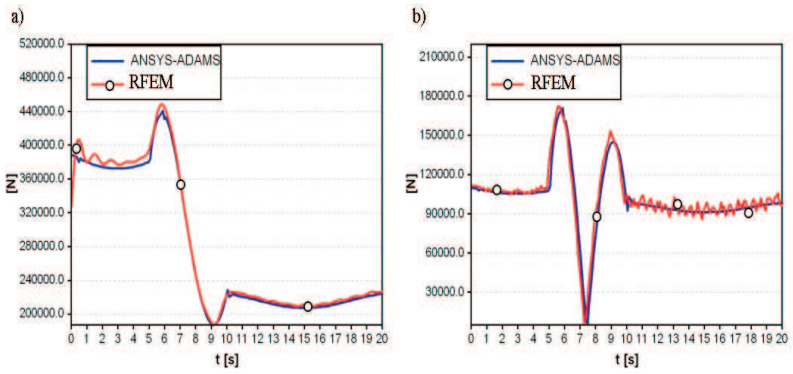

Fig. 12. Comparison of RFEM and Ansys-Adams models: a)vertical reaction in the A-frame leg; b) force in the servo-motor

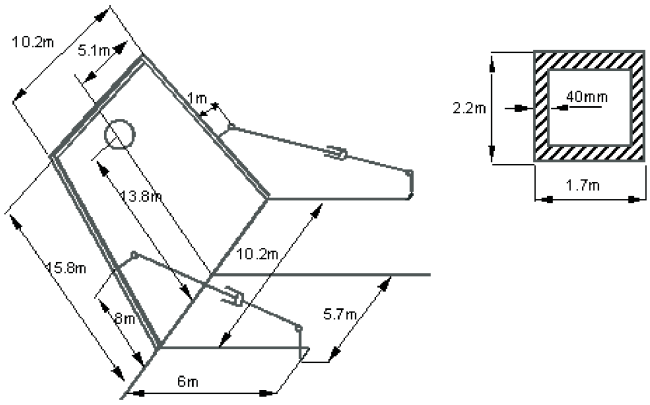

Fig. 13. Geometrical parameters of the A-frame

The value of load coordinates $x_{L,3}$, for which the optimisation process has been carried out is h=-300 m, mass of load m_L=100 Mg, and the motion of the ship is defined as:

$$\begin{cases} x_{c,1}(t) = 1\sin\left(\dfrac{2\pi}{6}t\right) \\ x_{c,2}(t) = 0 \\ x_{c,3}(t) = 2\sin\left(\dfrac{2\pi}{12}t\right) \\ \varphi_{x,1} = 0 \\ \varphi_{x,2} = 0 \\ \varphi_{x,3} = 0 \end{cases} . \tag{42}$$

In the figures, the following denotations are used: Ω_1, Ω_2 – curves obtained according to (31) and (32), respectively, S, H – curves obtained according to (33) and (34). Fig. 14 shows time courses of coordinate $x_{L,3}$ obtained according to the full (presented in section 2) and the simplified model. In this case, the hoisting winch was motionless. The results of simulations are almost the same.

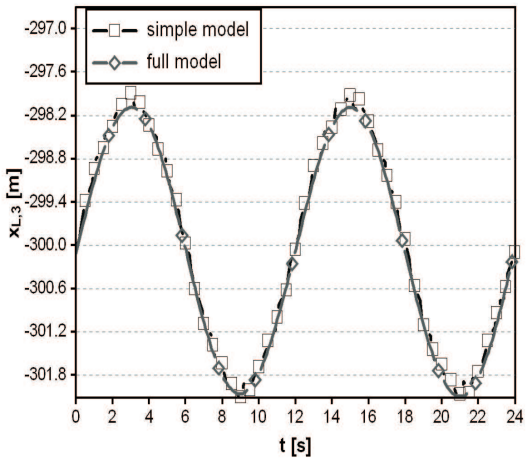

Fig. 14. Time courses of coordinates $x_{L,3}$

Because the simplified model is much more numerically efficient, the optimisation process has been solved for this model. Time courses of drive functions of the drum defined during the optimisation process are presented in Fig. 15.

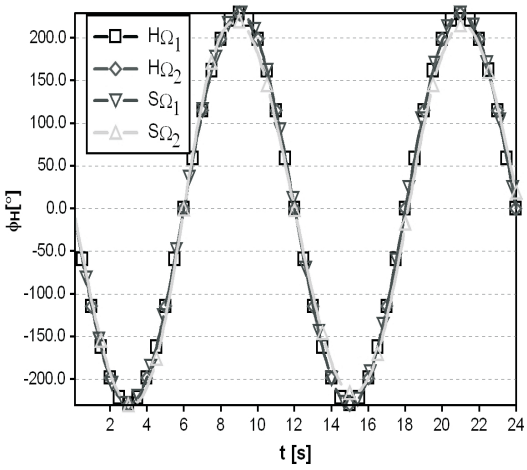

Fig. 15. Drive functions of drum after optimisation

As we can see, insignificant differences occurred between these drive functions. Drive functions obtained during optimisation have been taken as inputs of drum motion in the full model, so the simulations presented below have been carried out according to the model from section 2. Fig. 16 shows time courses of the coordinate $x_{L,3}$ obtained when the drum of the hoisting winch was motionless and when its motion was determined by function after optimisation (regardless of the type of the objective function and type of the drive function). The amplitude of load oscillations has been decreased from 2 m to near zero.

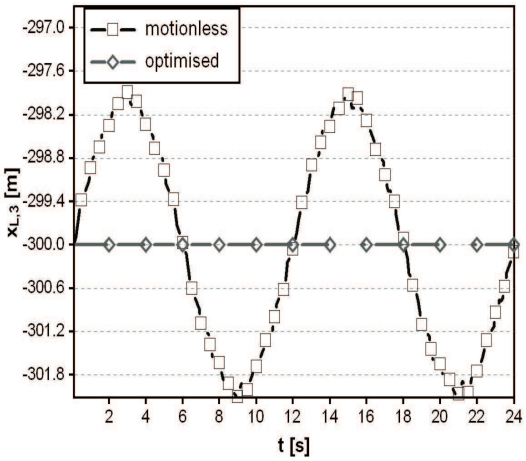

Fig. 16. Coordinate x_{L3} before and after optimisation

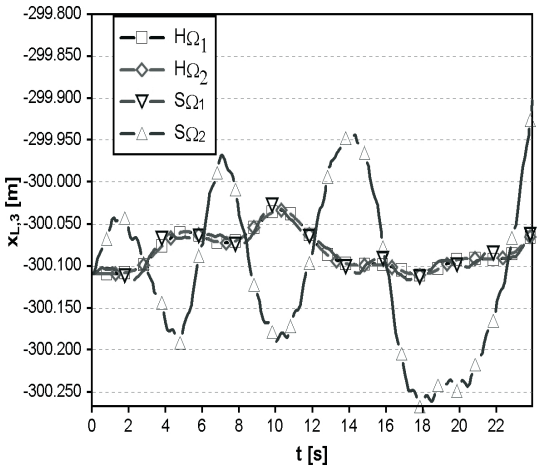

Fig. 17. Coordinate $x_{L,3}$ after optimisation for different type of objective and drive functions

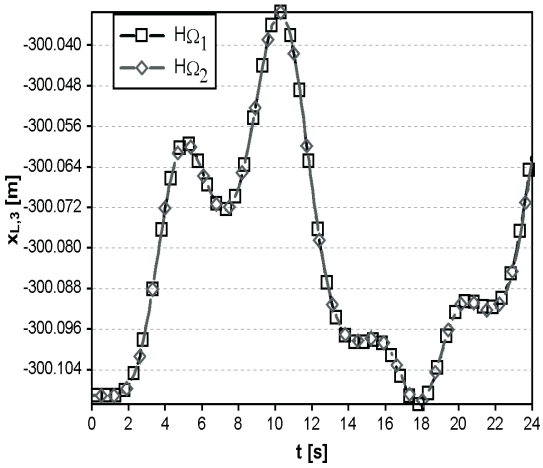

Fig. 18. Coordinate $x_{L,3}$ after optimisation for pseudo-harmonic drive function

Time courses of the coordinate $x_{L,3}$ obtained for different types of objective functions and drive functions are presented in Fig. 17. Fig. 18 presents in detail the courses for the pseudo-harmonic drive function (34) and different types of objective functions.

5. Final remarks

The model of an A-frame based on the rigid finite element method has proved to be a useful instrument for carrying out dynamic analyses of this kind of cranes. This model is more numerically-effective than the previous model presented in [5] – Fig. 3. In the new model, it is not necessary to take into account 12 reactions and respective equations of constraints.

Numerical simulations presented in the paper confirm the significant efficiency of the proposed method of optimisation of drive functions of the drum where the main goal of the optimisation process is the stabilisation of the load position. Because the optimisation task has been carried out for the simplified model, the method is sufficiently effective.

The drive functions of the hosting drum calculated for specific wave systems would be permanently stored in the A-frame control system memory (forming the so-called "map of basic drive functions"). Functions for other wave systems would be determined by the control system in real time, based on approximation. Of course, the wave system is not a single parameter which has to be taken into account. Mass of the load and length of the rope are particularly important. During the construction of the „map of basic drive functions", the knowledge of sensitivity of load stabilisation to these

remaining parameters is essential. This problem should be discussed in our future works.

For the motion of the ship discussed, the pseudo-harmonic drive functions are slightly better than spline functions. Amplitudes of load oscillations in the $x_{L,3}$ direction are, for pseudo-harmonic functions, about 8 times smaller then for the spline function and the objective function Ω_1. When the objective function Ω_2 is taken, the results obtained are worst. However, when the system of waves is more complicated, the spline functions may be more useful.

Both objective functions, that is the average and the maximal value of deviation of load position from the demanded level, are acceptable in practice. There are no significant differences between the results obtained for the two functions.

In real conditions, there are additional phenomena that can influence the quality of the stabilisation of the load position. There may be, for example, inaccurate definition of parameters of the crane. We should also remember that the rope interacts with the load and the environment mainly at low levels of depths, where water currents and waves are strong. Especially, in some conditions, a taut-slack phenomenon of a marine cable-body system can be significant [9], [10]. Vertical oscillations of the load induced by taut-slack phenomenon makes it more difficult to stabilise the load. An error-actuated control system for motion of the drum of the hoisting winch can minimise the impact of all those phenomena. Those problems will be addressed in our future research.

Manuscript received by Editorial Board, November 14, 2008;
final version, April 02, 2009.

REFERENCES

[1] Charpra S. C., Canale R. P.: Numerical methods for engineers: With software and programming Applications. McGraw-Hill, New York, 2002.

[2] Craig J. J.: Introduction to Robotics: Mechanics and Control (3rd Edition). Prentice Hall, 2003.

[3] Driscoll F. R., Lueck R. G., Nahon M.: Development and validation of a lumped-mass dynamics model of a deep-sea ROV system. Applied Ocean Research, 2000, 22, pp. 169-182.

[4] Ellermann K., Kreuzer E., Markiewicz M.: Nonlinear dynamics of floating cranes. Nonlinear Dynamics, 2002, Vol. 27, No. 2, pp. 107-183.

[5] Fałat P.: Dynamic Analysis of a sea crane of an A-frame type, Ph.D. Thesis, University of Bielsko-Biała, Bielsko-Biała, 2004 (in Polish).

[6] Fałat, P. Adamiec-Wójcik I., Wojciech S.: Application of the rigid finite element method to modelling dynamics of an Aframe. Proc. 8th Conference on Dynamical Systems Theory and Applications, Łódź, 2005, pp. 277-284.

[7] Fałat P., Gancarczyk T., Wojciech S.: Program for static load analysis of an A-frame. Proc. Euroconference On Compatational Mechanics and Engineering Practice, Szczyrk, 2001, pp. 144-149.
[8] Fałat P., Wojciech S.: Application of non-linear optimisation methods to stabilise motion of a sea probe. Zeszyty Naukowe, Budowa i Eksploatacja Maszyn, Akademia Techniczno-Humanistyczna w Bielsku-Białej, 2003, Ser. 4, z. 6., pp. 29-40.
[9] Huang S.: Stability analysis of the heave motion of marine cable-body systems. Ocean Engineering, 1999, 26, pp. 531-546.
[10] Jordan M. A., Bustamante J. L.: Numerical stability analysis and control of umbilical-ROV systems in one-degree-of-freedom taut-slack condition. Nonlinear Dynamic, 2007, 49, pp. 163-191.
[11] Kruszewski J., Sawiak S., Wittbrodt E.: Metoda sztywnych elementów skończonych w dynamice konstrukcji. WNT, Warszawa, 1999 (in Polish).
[12] Li, Y., Y., Balachandran, B.: Analytical study of a system with a mechanical filter. Journal of Sound and Vibration, 2001, 247, pp. 633-653.
[13] Maczyński A.: Positioning and Stabilization of Load for Jib Cranes. Wydawnictwo ATH, Seria Rozprawy Naukowe 14, Bielsko-Biała, 2005 (in Polish).
[14] Masoud Z., N., Nayfeh A., H., Mook D., T.: Cargo pendulation reduction of ship-mounted cranes. Nonlinear Dynamics, 2004, Vol. 35, No. 3, pp. 299-311.
[15] Wittbrodt E., Adamiec-Wójcik I., Wojciech S.: Dynamics of flexible multibody systems, Springer, 2006.

Stabilizacja ładunku w żurawiu morskim typu A-rama

S t r e s z c z e n i e

W pracy przedstawiono model dynamiczny żurawia typu A-rama. Do dyskretyzacji podatnej struktury (ramy) zastosowano metodę sztywnych elementów skończonych (SES). Zaproponowano zastosowanie metod optymalizacyjnych do określenia przebiegu funkcji napędowej wciągarki. Celem optymalizacji było zapewnienie stabilizacji położenia ładunku. Aby uzyskać zadowalającą efektywność numeryczną, zadanie optymalizacji rozwiązywano dla uproszczonego modelu A-ramy. Porównano wyniki obliczeń numerycznych uzyskanych dla różnych funkcji celu i różnych typów funkcji napędowych.